ESTIMATING PRELIMINARY OCCUPANT INJURY RISK DISTRIBUTIONS FOR HIGHLY AUTOMATED VEHICLES WITH RESPECT TO FUTURE SEAT CONFIGURATIONS AND LOAD DIRECTIONS

Felix Ressi
Wolfgang Sinz
Graz University of Technology
Austria

Claus Geisler
Abdulkadir Öztürk
Daimler AG
Germany

Gian Antonio D'Addetta
Heiko Freienstein
Robert Bosch GmbH
Germany

Paper Number 19-0175

ABSTRACT

While highly automated vehicles (HAVs) will be able to reduce the number of accidents significantly by removing human error, some accidents may remain unavoidable – particularly during the transition period. HAVs also promise increased freedom in seat positioning for all passengers, including the driver. A growing amount of literature deals with individual issues of occupant safety in these new positions, but there is currently no comprehensive overview on the effects of combinations of possible future seat positions and vehicle load directions. Addressing this, the aim of this research is to develop a method to quickly highlight key combinations of seat position/inclination and crash load direction with respect to occupant safety for any given interior layout and set of restraint systems. Also, the method should facilitate the evaluation of restraint systems' active principles. Inspired by common safety engineering methods, the proposed approach defines risk as combination of severity, exposure and controllability. To estimate the severity, each restraint system's ability to restrain the occupant – referred to as restraining potential – is defined as mathematical function of relevant parameters, e.g. various seat adjustments and as function of the load direction relative to the occupant. These individual restraining potential functions which can be plotted as 2D-graphs, can then be combined into a total restraining potential for any specific combination of parameters (seat, load direction...). The required interpolation points for these functions are estimated theoretically and checked for plausibility based on finite element (FE) simulations with a human body model (HBM) and compared to literature. Additionally, the space available for occupant displacement (and thus available for dissipation of kinetic energy) is considered and combined with the restraining potential to a measure which is inversely proportional to the severity. The exposure is estimated with a distribution of the main accident types (front/side/rear). While the relevant future distribution is not yet known, estimates from recent literature or current accident data can be used as starting points. With a modular approach, effects of different distributions can easily be analysed by changing this input. Controllability (with respect to the risk definition) is not taken into account in this first implementation, since the approach only considers scenarios where crashes occur and all systems are expected to work faultlessly. Based on the calculated severity and exposure the occupant injury risk is automatically computed for a specific interior and then plotted for all reasonable combinations of seat adjustments. This enables an immediate overview for finding key combinations which should be the focus of in-depth analyses, e.g. detailed FE simulations. The proposed approach should not be seen as a replacement for detailed FEA but as a useful supplement for time and resource efficient preparation of simulation studies concerning the occupant safety of future HAVs. Estimating preliminary occupant injury risks for future HAVs provides an insight to their expected performance which highlights key parameter combinations and can aid the development of relevant regulations and test procedures.

INTRODUCTION

Among other benefits, highly automated vehicles (HAVs) promise a significant reduction of the number of accidents. The important role of human error as accident cause is widely acknowledged but it is hard to determine the actual percentage of accidents which would be prevented if cars drove themselves. A study in 2008 suggested that over 90% of accidents are caused by human error [1], but even removing all human factors does not mean that the number of car crashes is going to be reduced to 10% – particularly not in the short or even mid-term. While the goal has to be to prevent all accidents, at least a significant reduction of accident numbers can be expected with

the introduction of HAVs. Especially accident causes like distraction, driving under the influence of alcohol or drugs, fatigue and cardiac and circulatory troubles – which together accounted for over 40% of all fatal crashes in Austria in 2017[1] [2] – could be removed completely. Still, considering that in 2016 the average vehicle age in the European Union was more than ten years and that as of today fully-automated driving is not available in a series production vehicle, it will take many years until all cars on the roads are HAVs. Particularly during the transition phase, unforeseeable circumstances or the mix of conventional and automated vehicles will produce scenarios in which the accident cannot be avoided by the HAV. In these remaining crashes new challenges for occupant safety emerge due to the increased spatial freedom HAVs can potentially offer to occupants. When the car takes over control and the driver is released from the driving task, he or she essentially becomes a passenger. Passengers in conventional cars are already spending the time during journeys on various other activities. In HAVs, all occupants could read, use their mobile devices, talk to one another, relax or even sleep while being chauffeured by the car. The standard driving position is not ideally suited for most of these activities – especially considering that the "driver" does not need to reach the controls, since the car is driving itself. In a qualitative study by Jorlöv et al. most participants expressed the desire to rotate their seats [3], at least for longer journeys, which suggests that passengers are potentially open to new interior layouts. These new possibilities have motivated many concepts for new seat configurations [4]. Most of these concepts have three ways of adjustments in common. Figure 1 shows a sketch of a seat with a vehicle coordinate system according to ISO 4130:1978 [5] and the three main adjustments: seat rotation β, increased backrest inclination α and longitudinal adjustment ΔX towards the rear of the vehicle.

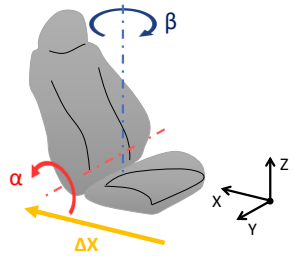

Figure 1. Main seat adjustments for new spatial configurations in HAVs (CS according to ISO 4130:1978).

These new seat configurations motivate a new area of research in the field of occupant safety. While there are many crash test configurations required by laws, regulations or performance assessment programmes for conventional seat configurations around the world, there are currently no mandatory crash tests specifically addressing the possible new seat configurations in HAVs. Instead of establishing mandatory tests, the United States Department of Transportation (US DOT) and the National Highway Traffic Safety Administration (NHTSA) encouraged car manufacturers to demonstrate due care to ensure full protection of all occupants in its Federal Guideline on Automated Driving Systems [6].

In absence of concrete rules or regulations, the key to demonstrate such due care is to determine all relevant load cases for such vehicles and to provide sufficient evidence that all occupants – when exposed to these load cases – experience acceptable injury risks. One way to approach this is to consider two perspectives: external and internal. The external perspective accounts for all external factors affecting the crash-induced loads on the occupants. Equivalently, the internal perspective accounts for all factors inside the vehicle. All of these factors need to be considered since they form the basis of any occupant injury risk assessment – the crucial part of demonstrating due care. Figure 2 illustrates this approach.

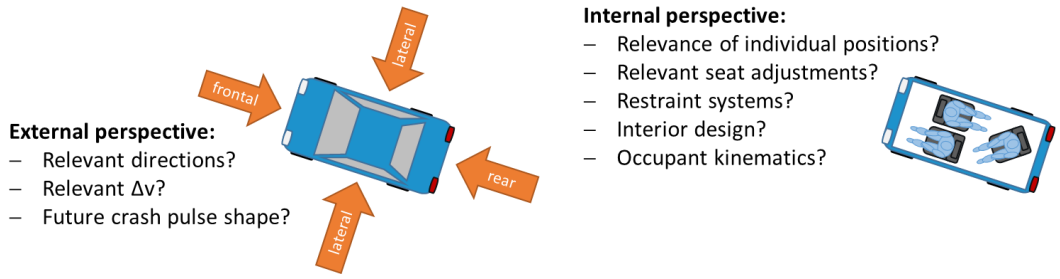

Figure 2. Illustration of the external and internal perspective affecting the loads on an occupant in a HAV.

[1] This number should be seen as an estimation, since it is derived from accident reports forms, compiled by police officers at the accident site. Even if subsequent analyses, e.g. by accident investigators, reveal a different accident cause, the original accident report is often not updated accordingly.

The external perspective encompasses the relevant future impact directions, the kinetic energy of the impact (commonly estimated with the velocity difference pre-/post-collision, Δv) and the shape of the crash pulse, which is the result of the HAV's stiffness and the stiffness of the striking vehicle. All these factors can only be estimated, since highly automated cars are not commercially available yet. Consequently, hardly any field data is available. While data from conventional vehicles can be used, it should be seen as an indication and be updated as soon as new research or data is available. Favarò et al. [7] found that out of 26 crashes involving HAVs in California between September 2014 and March 2017, injuries where only reported in two cases. They also provide a damage distribution for the HAVs, where rear damage accounts for the majority of 62%. Side and front damage only make up 23% and 15% respectively. While the study provides an interesting first glimpse at the issue, the empirical value of the accident distribution must not be overestimated, particularly because it only covers a very limited number of cases. It is only used in the present study exemplarily to provide a starting point.

The internal perspective (see right hand side in Figure 2) depends, to some extent, on the environment. For instance, the importance of a specific restraint system like the curtain airbag for reducing the occupant injury risk is dependent on the load case. In this case, the curtain airbag's importance is much higher in lateral impacts than for example in rear-end crashes. Nevertheless, there are many aspects of the internal perspective which are not reliant on external factors. Examples are the relevance of seat configurations in terms of acceptance by passengers of HAVs or the future interior designs as showcased by many OEMs and suppliers in concept vehicles. This is important since it defines the adjustment ranges of the seat system and the interior layouts which are relevant for further analysis. Since ultimately the focus of the internal perspective is the occupant and specifically it's injury risk for all relevant seat configurations it should be discussed in more detail.

In principle, there are two main approaches to estimate occupant injury risks for a given vehicle concept. One way is physical testing of prototypes e.g. with a sled test setup. Anthropomorphic test devices (ATDs) can be used in these tests to represent and measure the human response to the applied crash loads. While this approach is commonly used in later stages of development, it is often too costly and time-consuming to use it in pre-development, where many configurations need to be evaluated. The alternative, virtual testing, offers many benefits particularly in terms of flexibility and the ease of use for evaluation of large numbers of configurations (once the models are built). Even the Federal Guideline on Automated Driving Systems explicitly states that the demonstration of due care need not be limited to physical testing but may also include virtual vehicle and human body models[2] (HBMs) [6]. Using HBMs in the context of alternative seat configurations is especially interesting for four main reasons, which are discussed in the following paragraphs.

Firstly, commonly used ATDs or crash test dummies were designed to be used in upright seat configurations, as they are for instance defined in current laws and regulations. Many new concepts for future vehicles promote "relax" or "lounge" positions with significantly reclined seatbacks [9–11]. These positions are generally infeasible with state of the art dummies due to the non-adjustable angle between their thighs and their torso. HBMs can theoretically take any position a human can, even if this usually is a time-consuming task.

Secondly, unlike commonly used crash test dummies, most HBMs are validated for multiple loading directions. The dummy used in most frontal crash tests, the Hybrid III 50th percentile male, is only calibrated with frontal crash loading [12]. Likewise, the state-of-the-art side and rear impact ATDs, the WorldSID and the BioRID II, are only validated for lateral (±30°) [13] and rearward impacts respectively [14,15]. The latest frontal ATD, the "Test Device for Human Occupant Restraint", or short THOR, has also not been designed for multi-directional use [16], but could be modified to be comparable to dedicated side impact dummies [17]. While it might currently be the ATD most suited for multi-directional use, it is only validated for frontal impacts [18]. By contrast, state-of-the-art HBMs like the Global Human Body Model Consortium (GHBMC) models or the Total HUman Model for Safety (THUMS) are validated on component and regional level as well as for whole body impacts from various directions [19–22]. This means, they are theoretically able to predict injuries independently of the loading direction [23], which is particularly useful when comparing the effects of seat rotation angles that result in a combination of frontal and lateral loading on the occupant. Their biofidelity depends almost exclusively on the validation quality and is theoretically not limited by design, like in ATDs, where loads can only be measured in sensor positions and often only one loading direction.

Thirdly, human body models offer the possibility to represent human diversity far more accurately than ATDs. Many crash test dummies are only available in one or only a small number of size and weight specifications

[2] Throughout this paper the term 'human body model' refers to models considering the complex human anatomy including a full skeleton, adopting Euro NCAP's definition in their technical bulletin on Pedestrian Human Model Certification [8].

(usually derived from the 50th percentile of a sample population). HBMs can be morphed to represent any individual in terms of anthropometry, body mass index and even age [24].

Fourthly, some HBMs offer the possibility to model muscle activity, also referred to as active human body models (A-HBMs) [25,26]. Muscle activity is most significant during low-g loading conditions like emergency braking or swerving manoeuvres. ATDs passive models and also only validated for high-g loading and therefore not usable under low-g loading conditions. Yet, these scenarios are particularly relevant for HAVs, because if an unavoidable crash is detected by the vehicle, reversible and irreversible safety features could also be deployed before the actual crash itself. This calls for high accuracy occupant models for the pre-crash phase. [27]

While these benefits make HBMs a very interesting option for research in the area of occupant safety for HAVs, there are currently some disadvantages to be considered. The detailed representation of the human body comes at the expense of increased computational resources. State-of-the-art finite element models of HBMs have between 1.9 and 2.5 million elements [25] whereas detailed virtual dummy models have around 0.3 to 0.5 million elements [28,29]. This increases simulation times significantly and automatically raises the computational demands for data storage and post-processing. The other main drawback of HBMs compared to dummies is that results obtained with these simulation models cannot be tested or validated in the physical world directly. Also, while detailed injury analysis is one of their main advantages, more research is needed on strain-based assessment methods. Many body regions are still lacking reliable injury risk functions [30] including the lumbar spine. This body region could become more important for HAVs, since it is going to be subjected to more loading in more reclined seat positions (increased spine compression). Nevertheless, due to the unique insights they can give into kinematics and possible sources of injury, they are an important tool in the current and future occupant safety assessment of HAVs.

Recently, many publications have dealt with various aspects of occupant safety in HAVs and used different models in the process. Table 1 compares these simulation studies with regard to the occupant model and the parameters which were used for variation. In this table, the algebraic signs of all adjustments refer to the sketch in Figure 1, not to the convention used in the individual publications.

Table 1.
Comparison of current literature on occupant safety in HAVs.

Publication	Occupant model	α	β	ΔX	Impact		Interior	Belt routing[3]	Restraints[4]
				[mm]	Dir.[5]	Δv $\left[\frac{m}{s}\right]$			
Kitagawa et al. 2017 [31]	THUMS v4	base	0°, -30°, 180°	-	F	15.56, 11.1, 8.3	yes	D/P	3P-B
		24°, 36°, 48°	0° - 360° (45° steps)				no	D	
Jin et al. 2018 [32]	THUMS v4	base	0°, 90°, 135°, 180°	-	F	15.56	no	D	3P-B
Huf et al. 2018 [33]	THOR	fully reclined	0°	-	F	?	only for β = 180°	D	3P-B, SEMS
	H III 5th	base, fully reclined	0°, 180°						active head & backrest, SEMS
	H III 50th								
	THUMS v3								
	ES2	base	90°						3P-B, CC-B, SIP
Gepner et al. 2018 [34,35]	GHBMC O	25°, 45°, 60°	0°, 30°, 90°, 135°, 180°	-	8[6]	?	yes	P	3P-B, PAB, CAB, SAB
	GHBMC OS								
	THOR	25°, 45°							
Zhao et al. 2018 [36]	GHBMC O	base	0° - 360° (30° steps)	-	F	11.1	no	D	3P-B
Boin 2018 [37]	H III 50th	base	0°, ±30°, ±45°	-	F	16.2	no	D	3P-B, CC-B, Airbelt, improved seat and headrest
	ES2-re		60°, 90°		F	11.1			

[3] P – passenger side (in conventional vehicles), i.e. shoulder belt routed from the right shoulder to the left side of the pelvis; D – driver side, i.e. shoulder belt routed from the left shoulder to the right side of the pelvis.
[4] 3P-B – 3-point-belt; CC-B – criss-cross-belt; PAB – passenger airbag; CAB – curtain airbag; SAB – side airbag; SIP – side impact pad for head, thorax and pelvis; SEMS – seat energy management system.
[5] Impact direction w.r.t. the vehicle (F – front, S – side, R – rear).
[6] Eight impact directions: 0°, ±30°, ±90°, ±150°, 180° with moving deformable barrier, v = 15.56 m/s.

While most of these publications consider the effects of individual seat configurations on occupant kinematics (and sometimes injury risk), there is currently no comprehensive overview on the effects of combinations of future seat configurations under various impact directions. It would be theoretically possible to estimate the effects of changing one parameter based on expertise but changing four parameters at once quickly leads to an unmanageable situation. Therefore, setting up finite element analyses (FEA) is the preferred method. The main issues with this approach are the lack of finite element models which are validated for all the relevant loading conditions and the enormous number of possible combinations. While it is possible to simulate hundreds of combinations individually, finding an efficient approach to prioritise or identify the most relevant ones from an occupant safety perspective could reduce the computational costs and time significantly. Many disciplines are faced with similar tasks of identifying the most significant combination of parameters among a large number of possible combinations. Well known examples for such methods in the area of reliability engineering are the failure mode and effects analysis or the hazard analysis and risk assessment described in ISO 26262 [38]. Theoretically, this could also be an area of application for the growing field of machine learning.

The main objective of the present study was to develop a method to quickly highlight key combinations of seat configurations and crash load directions with respect to occupant safety for any given interior layout and set of restraint systems. Additionally, the method should facilitate the evaluation of restraint systems' active principles. The considered parameters are the seatback inclination (14 discrete angles), the seat rotation (13 discrete angles) and the longitudinal seat adjustment (4 adjustment positions). These are combined with three load cases (front, side and rear crash) to estimate an occupant injury risk for every combination. Multiplying all parameter ranges with one another, this results in 2184 possible combinations. Out of these, all variants with a higher risk value should be prioritised and be the focus of further investigation. Also, some configurations, while being theoretically possible, might not be technically feasible and are actually irrelevant in practise. In this case, the configuration – despite potentially having a high risk value – should be excluded from further analysis and not made available in future vehicles.

METHOD

The general approach to estimate the occupant injury risk distributions is illustrated in Figure 3. First, the seat configuration and vehicle characteristics have to be defined. This information is used to look up the relevant (pre-defined) restraining potentials and compute the available distance to interior surroundings. Similar to the hazard analysis and risk assessment in ISO 26262 [38], the severity can then be estimated and combined with the measures for exposure and controllability to the risk estimate. In this first implementation, controllability is not taken into account, since only scenarios where crashes occur are considered and all systems are expected to work faultlessly.

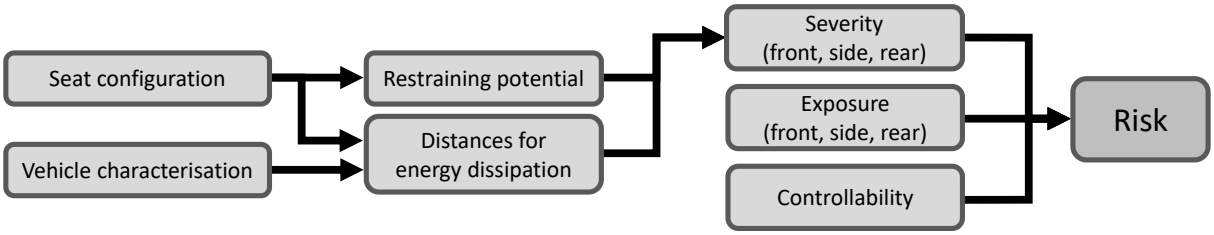

Figure 3. Schematic overview on the general approach to estimate the occupant injury risk distributions.

With respect to the internal/external perspective, this approach focusses mainly on the internal perspective. In this first step, a separate investigation makes sense – in particular to assess the main challenges. Also, at this stage, many factors regarding future accident scenarios are still unknown. The external factors, which are necessary to assess occupant safety within the internal perspective (in particular the accident distributions to estimate the front/side/rear exposure levels), are determined using recent literature. Where this is not possible the factors are estimated with a safety margin following a due care approach. For instance, the future crash severities for HAVs are unknown today, but it could be argued that they will be lower than the severity for conventional vehicles, due to their inherent lack of inattentiveness and lower reaction times. These reduced reaction times would in turn lead to lower collision velocities and hence lower crash severities. Therefore, while the currently mandated crash test severities represent an upper limit which represent a worst case scenario for this study, these are highly relevant for a due care approach.

The following paragraphs explain the individual aspects illustrated in the overview in Figure 3 in more detail.

Seat configuration

The basis of the seat configuration is made of the three adjustments introduced in Figure 1 (seat rotation β, increased backrest inclination α and longitudinal adjustment ΔX). While occupants can theoretically take many

different postures in one seat position, it is assumed, for the purpose of this study, that the occupants H-point matches the equivalent H-point that has been determined for the seat. For reasons of simplicity, this point is also defined as the base point for the seat rotation (angle β) about the Z-axis. Furthermore, the occupant's torso is assumed to be in contact with the backrest and asymmetric postures are not considered. While many activities which are possible in HAVs will involve the occupants holding objects in their hands (mobile devices, books, etc.), a relaxed arm position is assumed (i.e. hands in lap) to reduce the number of variables.

To facilitate future comparisons of configurations with different load cases but similar direction of loading with respect to the occupant the load direction φ is defined. Figure 5 illustrates the relationship between the seat rotation β and the load direction with respect to the occupant φ. For a frontal collision, φ equals β (illustration on left side of Figure 4). For the lateral load case, when the vehicle is struck from the left side (illustration in the middle of Figure 4), φ is defined as $\beta + 90°$. Equivalently, in the rear crash load case, φ is defined as $\beta + 180°$ (illustration on right side of Figure 4).

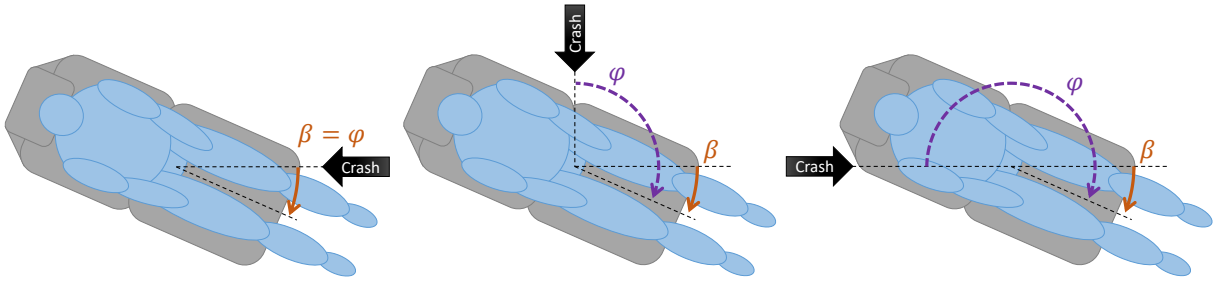

Figure 4. Illustration of the relationship between the seat rotation β and the load direction φ.

To estimate if intersections with the interior occur, parameters describing the seat, its position and its space requirements need to be defined. The most extreme extensions of the seat in X and Y direction, relative to the base point (the H-point), are determined in the following way. The distance between the 50th percentile occupant's pelvis to the head, d_{HP}, is used in combination with the backrest inclination α to calculate the theoretical position of the head-COG (cf. illustration on the left side of Figure 5). From this point, the parameters w_{SB} (width of the seatback at the rear) and d_{HS} (distance between the 50th percentile's head-COG and the back of the seat), shown in the illustration in the centre of Figure 5, are used in combination with the seat rotation β to approximate the two distances s_{S_lat} and s_{S_lon}. These two distances are shown in the illustration on the right of Figure 5.

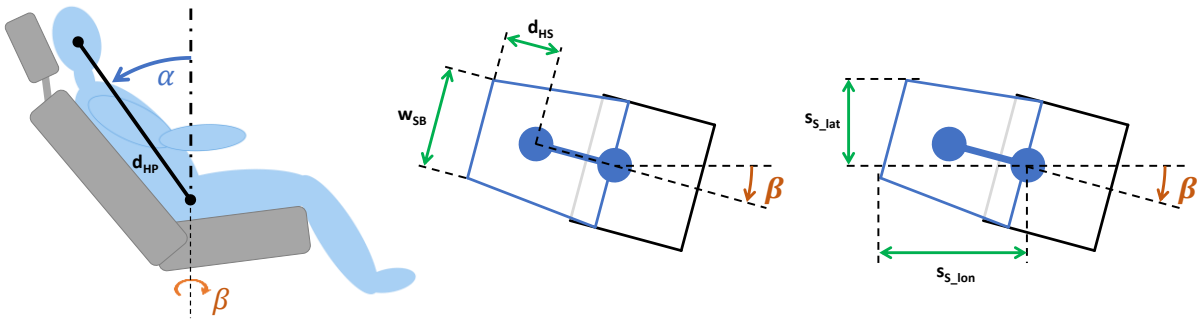

Figure 5. Illustration of the parameters describing the seat configuration and its space requirements.

Vehicle characterisation

To characterise the vehicle, the load cases and the interior dimensions, a number of parameters have to be defined. Also, some general information about the available restraint systems needs to be determined. The restraint systems in the vehicle discussed in the present study are summed up below:

- Standard vehicle seat
- Seat integrated 3-point belt system (with pretensioner and load limiter)
- Frontal airbag (fixed to the vehicle, in other words: independent of seat position)
- Side airbag (seat mounted)
- Curtain airbag (fixed to the vehicle, in other words: independent of seat position)

Figure 6 shows a top view of a vehicle seat, rotated 15° clockwise (angle β) and the distances (green arrows) of the seat H-point to the interior (grey dashed lines). Distance s_{BP_Y} indicates the available space between the seat

H-point and the lateral interior, while s_{BP_X} and s_{BP_-X} indicate the space to the rear and the front of the interior respectively. The longitudinal distances obviously change when the seat is moved to a more rearward position, therefore the distances have to be defined in a base position (which is the standard driving position).

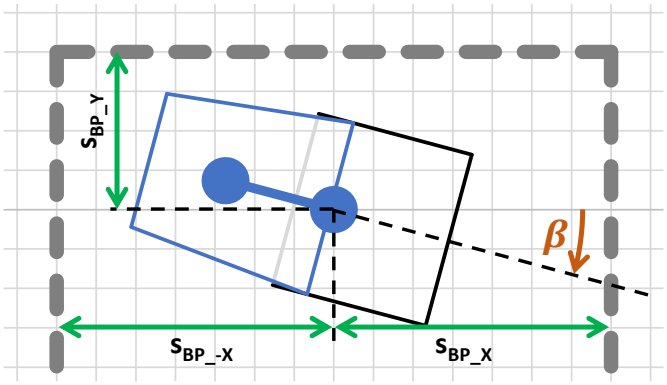

Figure 6. Schematic vehicle seat and interior (top view) with the distances describing the seat position.

These distances, together with the seat rotation, the recline angle and occupant size make it possible to estimate the distances of the occupant's head to the interior – which, in combination with the crash velocity, is later used to determine a theoretical mean deceleration for each load case.

Additionally, these distances are utilized to determine if a certain combination of seat adjustments is feasible in the given interior space around the base position. The example in Figure 7 illustrates that with increased seat rotation, the distance s_{SB_lat} between the seatback and the lateral interior is reduced. Likewise, if the seat is moved towards the rear, distance s_{SB_lon} between the rear of the seat and the interior is reduced. For large enough rotation angles or excessive longitudinal seat adjustments towards the rear the seat would collide with the interior. Configurations which lead to such collisions are not evaluated since they are irrelevant in practise.

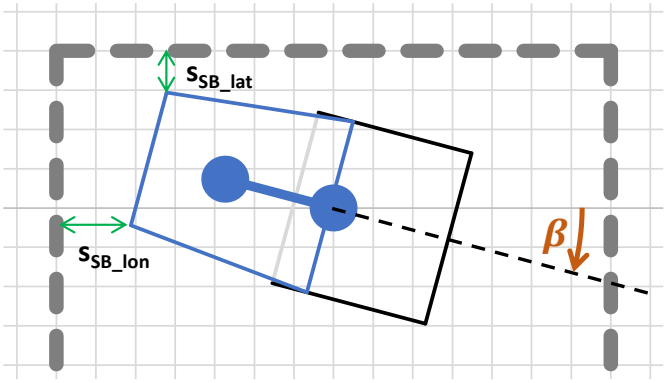

Figure 7. Schematic vehicle seat and interior (top view) with distances between seat and interior.

In addition to these geometric parameters, the load cases have to be defined. The load cases used in the present study consist of a frontal, a lateral and a rear crash, which are characterised by their Δv. The crash severity representing the frontal collision is derived from a full-width crash test with 56 km/h into a rigid wall. Accordingly, the severity for the lateral impact is represented by a crash test with a deformable barrier which is striking the vehicle with a speed of 55 km/h (normal to the vehicle). While a pole crash test is generally the more demanding lateral load case in terms of occupant safety due to its inherently larger intrusions, it is not deemed representative for HAVs. The reason for this is the assumption that the systems in a HAV will be designed in a way that running off accidents (and subsequent lateral collisions with trees or poles) will be avoided. The rear crash is represented by a test mandated for fuel system integrity. In this test a deformable barrier, moving at 80 km/h, strikes the vehicle from the rear. It can be argued that this represents a scenario, where the HAV is struck from behind by an inattentive driver of a conventional vehicle. Since all of these are standard crash tests for conventional vehicles, each represents a kind of upper limit considering the crash severities for HAVs.

Table 2 gives an overview of the defined parameters. The values for the parameters used in the present study can be found in the appendix.

Table 2.
Parameters used to characterise the vehicle interior and load cases.

Parameter	Symbol	Found in	Unit	Comments
occDistHeadPelvis	d_{HP}	Figure 5	m	Distance H-point to COG head[7]
spaceBasePositionX	s_{BP_X}	Figure 6	m	Initially available deceleration space - frontal
spaceBasePositionY	s_{BP_Y}	Figure 6	m	Initially available deceleration space - lateral
spaceBasePositionMinusX	s_{BP_-X}	Figure 6	m	Initially available deceleration space - rear
spaceAvailableY	s_{BP_Y}	Figure 6	m	Available space to the side (for seat rotation)
seatDepthBehindHead	d_{HS}	Figure 5	m	Distance between COG head and rearmost part of the seat
seatBackWidth	w_{SB}	Figure 5	m	Seatback width (at rearmost part)
velocityFront	-	-	m/s	Impact velocity - frontal
velocitySide	-	-	m/s	Impact velocity - side
velocityRear	-	-	m/s	Impact velocity - rear

In short, these parameters are used to estimate if a certain seat configuration is feasible in the proposed interior space and to calculate theoretical mean deceleration levels for the various impact conditions for the risk definition.

Risk definition

The risk definition consists of three elements: severity, exposure and controllability. This concept is loosely based on the risk definition used in ISO 26262 [38]. The most complex aspect is defining the severity in a way which is universal but selective. In other words, it needs to be applicable to all seat configurations while accurately distinguishing differences in potential injury severity between them. In this study, the severity is estimated in the following way. Each restraint system's ability to restrain the occupant – referred to as restraining potential – is defined as mathematical function of relevant parameters. A value of 100% means that the occupant is restrained perfectly just by this single restraint system while 0% means that the occupant is not restrained at all by the considered restraint system. Specifically, this is defined as a function of seat adjustments (recline angle and seat rotation) for every impact direction (front, side, rear). Figure 8 shows the restraining potential (RP) of the seat in a frontal impact as an example. The two plots on the left show the RP as a function of the seat rotation at 25° and 90° recline angle. The two plots on the right show the RP as a function of the recline angle at 0° and 180° seat rotation.

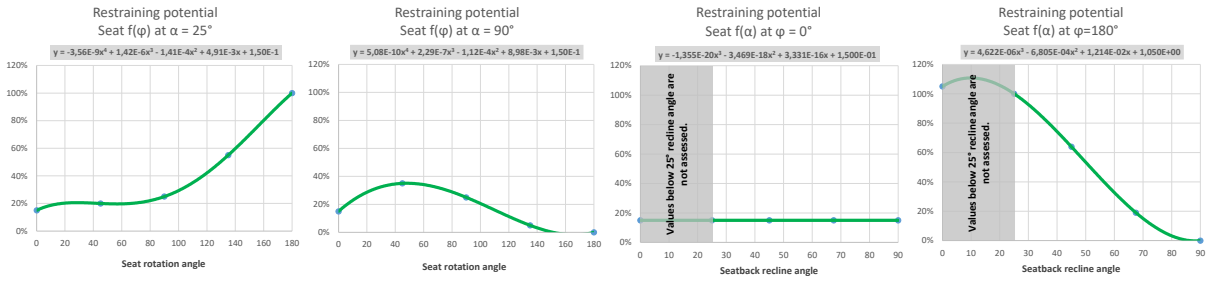

Figure 8. Restraining potential of the seat as a function of recline angle and seat rotation.

The first graph to the left shows that the RP of the seat increases with increasing seat rotation angle. This is based on the fact that with increased area to hold the occupant in position, the seats potential to restrain it is higher. While this is true for a base backrest recline angle of 25°, this is not the case for a fully reclined backrest (second graph from the left in Figure 8). In this configuration, the RP first increases until the seat is rotated 45°, which is the position that is estimated to produce the largest projected contact area between the seat and the occupant. This estimation is based on the assumption that at 45° seat rotation, this contact area comprises of a combination of the seat cushion itself (which is slightly angled backwards) and the side bolsters. For rotation angles above 45°, the RP decreases, because the projected contact area of the seat cushion is reduced, until it is negligible for 180°. It is important to note, that this is only valid for a seat for which the cushion angle is independent of the backrest angle. The second graph from the right shows that the seat's RP is independent of the backrest angle for 0° seat rotation. For 180° of rotation, the RP decreases with increased backrest recline, as the projected contact area is reduced. These curves represent a preliminary implementation which, while checked for plausibility with literature and

[7] This distance is occupant specific. The approximated measures for the Hybrid III dummy family are listed here as an orientation: H305: 590 mm; H350: 670 mm; H395: 704 mm

interim FEA, is subject to be updated in the future. Also, due to the smooth functions, this approach cannot account for phenomena like submarining, which do not occur gradually. Therefore, such effects need to be accounted for separately.

The four curves shown in Figure 8 essentially define the boundaries of a three-dimensional area diagram with the horizontal axes being seat rotation and recline angle, and the vertical axis representing the restraining potential of the seat. Figure 9 shows a plot of this area diagram, where the points between the boundaries are the result of linear interpolation of the four curves. The higher the area in the diagram, the higher the ability of the seat to restrain the occupant. The values, on which this plot is based, form a look-up-table which gives the restraining potential for the seat for any given parameter combination.

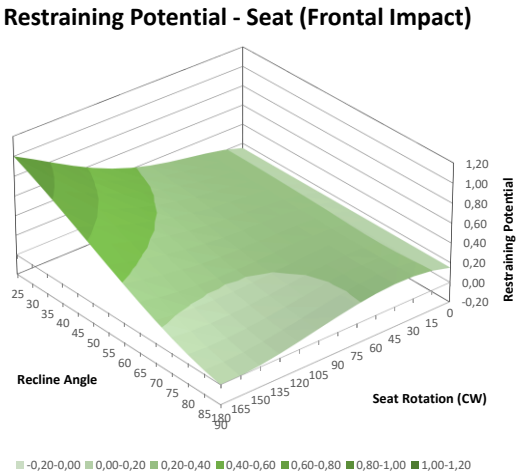

Figure 9. Restraining potential of the seat for frontal impacts as 3D-plot.

The restraint potential is also defined for the lateral and the rear impact condition, resulting in three look-up-tables per restraint system. The whole procedure is applied to the other restraint systems as well – resulting in restraining potentials of the 3-point seatbelt, the frontal airbag, the (seat mounted) thorax airbag and the curtain airbag in all three impact conditions.

The second element of the severity definition considers the estimated distance between the occupant's head and the closest interior parts in the direction of impact. This, together with the assumed impact velocity for each load case, enables the calculation of a mean deceleration. Figure 10 shows a diagram of an occupant in top and side view. The horizontal distance between the head and the pelvis (purple line) only depends on the recline angle α (which is approximated to be identical to the seatback recline angle).

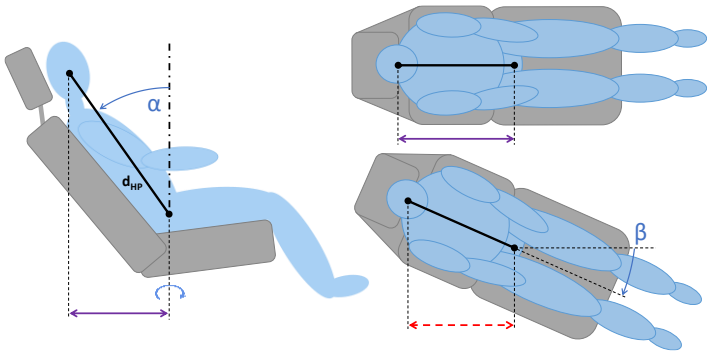

Figure 10. Top and side view of an occupant illustrating the calculation of the longitudinal distance between the head and the seat base point.

Accounting for seat rotation of β degrees about the vertical axis through the hip point, it is possible to calculate the longitudinal distance between the head and the seat base (rotation) point (red dashed line). This enables the estimation of the distance between the occupant's head and the interior for each impact direction. Figure 11 shows this in the form of a simple illustration for a frontal impact, the green distance s representing the total horizontal distance between the head and the interior.

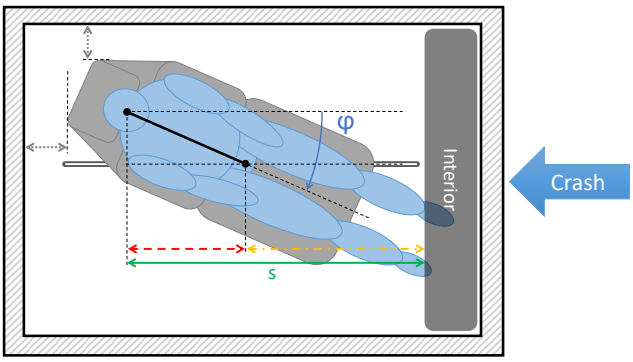

Figure 11. Illustration of the distance s between the occupant's head and the interior for a frontal impact.

This distance s is calculated for each seat configuration. Together with the assumed velocity v for each load case it can be put into Equation 1 to get an estimate of the mean deceleration $\bar{a}$. This is based on the theoretical assumption of uniform linear deceleration for the occupant.

$$\bar{a} = \frac{v^2}{2 \cdot s} \qquad \text{(Equation 1)}$$

Finally, for each individual parameter combination and load case, the quotient of the mean deceleration $\bar{a}$ and the combined restraint potential RP (which is the sum of the individual restraining potentials) equals the severity S (Equation 2).

$$S = \frac{\bar{a}}{RP} \qquad \text{(Equation 2)}$$

More distance in Equation 1 yields a lower mean deceleration and hence a lower severity. Nevertheless, increased distance to those restraint systems which are fixed to the vehicle and therefore do not move with the seat (e.g. the frontal airbag or curtain airbag) is generally not beneficiary. To account for this in the severity value, a modifier is included. If the distance between the head and the restraint which is relevant for the load case exceeds a "maximum range" threshold s_{range}, the modifier is activated. For positions where the distance s is larger than the threshold s_{range}, the adjusted severity S_{adj} is increased linearly, as shown in Equation 3.

$$S_{adj} = \frac{\bar{a}}{RP} + x_{mod} \cdot (s - s_{range}) \qquad \text{(Equation 3)}$$

To make this equation mathematically sound, the modifier has to have the unit s^{-2}, because RP is given in percent and therefore has no units. Since units are not relevant in this context and relative comparisons are more interesting, all the individual severity values are divided by the value obtained for the base seat configuration (cf. Equation 4). This means that in the resulting tables, a severity value of 1 indicates that the severity is equal to that in the base position. Lower and higher values identify reduced and increased severity respectively.

$$S_{norm\_R_{\alpha,\beta}} = \frac{S_{adj\_R_{\alpha,\beta}}}{S_{adj\_R_{0°,25°}}} \qquad \text{(Equation 4)}$$

The normalised severity measure on its own enables the comparison of all relevant seat configurations within one impact direction (examples are shown in Figure 12, Figure 13 and Figure 14). To evaluate the overall risk, exposure and controllability need to be addressed. The exposure is estimated with the distribution of the main accident types (front/side/rear). While the relevant future distribution for HAVs is not yet known, current accident data can be used as a starting point. Effects of different distributions, e.g. for different vehicle types or road types, can easily be analysed by changing this input. Controllability (with respect to the risk definition) is not taken into account in this first implementation, since we only consider scenarios where crashes occur and all systems are expected to work faultlessly (as mentioned in the beginning). Equation 5 shows the formula to calculate the risk which combines the severity of a given seat configuration for each impact direction with its respective exposure E_i.

$$R_i = \sum_{i}^{k} S_{norm\_R_i} \cdot E_i = S_{norm_{front}} \cdot E_{front} + S_{norm_{side}} \cdot E_{side} + S_{norm_{rear}} \cdot E_{rear} \qquad \text{(Equation 5)}$$

The formulas above were put into spreadsheets and severity and risk values were calculated for every possible parameter combination.

RESULTS

To get a clearer picture of the underlying effects, the severity charts are discussed individually, before their combination into the overall risk chart which is based on Equation 5.

Figure 12 shows the severity for a frontal impact for two longitudinal seat positions. The chart on the left side shows the severity for the base position; the chart on the right shows the severity for a seat positioned 300 mm towards the rear. The values are relative to the frontal severity in the standard position, which is defined as 0° seat rotation and 25° backrest inclination. Therefore, the frontal severity for this configuration is always 1,0, which stands for the base severity (see top left corner in Figure 12).

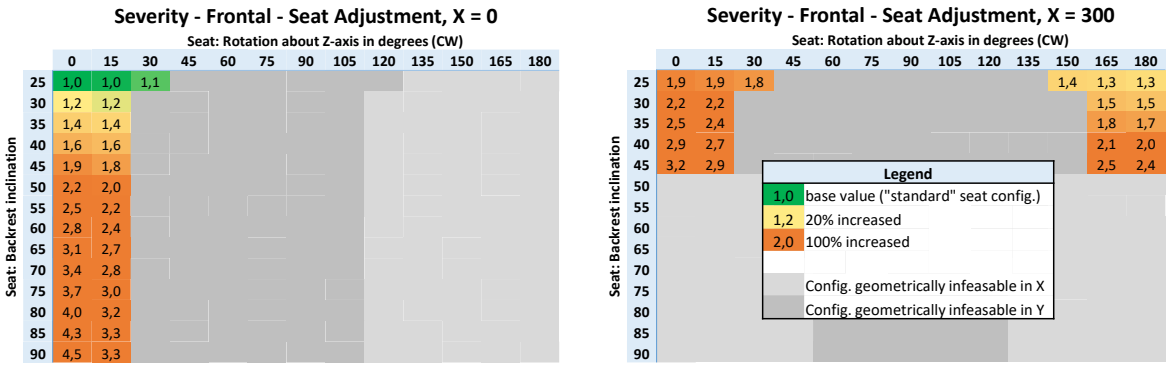

Figure 12. Severity for a frontal impact for two longitudinal seat positions (left: base, right: 300 mm rearward).

The legend on the right side of Figure 12 explains the colour codes. Green values are lower or equal to the base value of 1,0. Yellow values are 20% increased relative to the base position and orange values indicate a risk increase by at least 100%. The light grey areas indicate positions which have not been evaluated because they are not feasible in the given longitudinal vehicle interior space. Areas which are coloured in a darker grey have not been evaluated because there is not enough lateral space in the interior to realise the individual seat adjustment. For instance, in a seat position which is moved 300 mm further rearwards the backrest cannot be reclined as far much as in the base position. On the other hand, for the more rearward adjustment the seat can be positioned in a fully rotated configuration, since – due to the increased distance – the seat back clears the interior in the front of the vehicle.

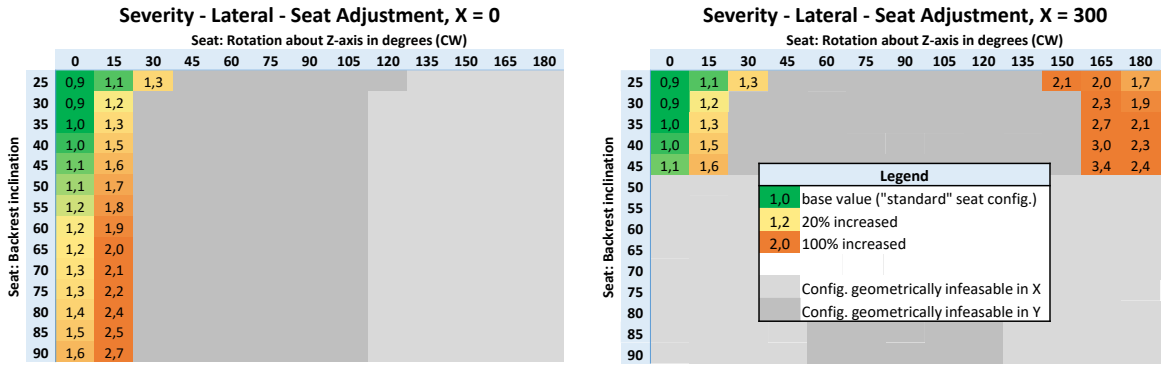

Figure 13. Severity for a lateral impact for two longitudinal seat positions (left: base, right: 300 mm rearward).

Since the interior dimensions do not depend on the load case, the same greyed out areas mark the configurations which are geometrically infeasible.

The equivalent charts for a rear impact load case are shown in Figure 14.

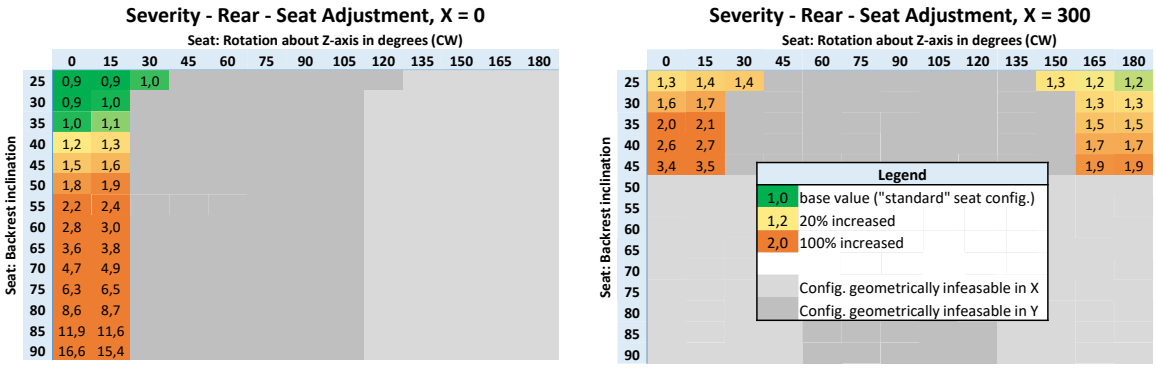

Figure 14. Severity for a rear impact for two longitudinal seat positions (left: base, right: 300 mm rearward).

Utilising Equation 5 and the exposure estimation (62% frontal, 23% lateral and 15% rear crashes) based on the accident data for HAVs by Favarò et al. [7], these severity charts can be combined to the exemplary overall risk charts shown in Figure 15.

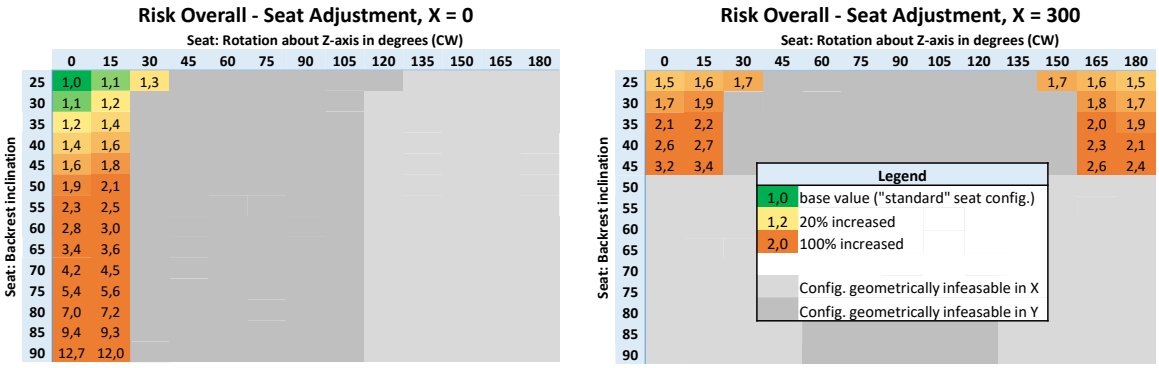

Figure 15. Overall injury risk for two longitudinal seat positions (left: base, right: 300 mm rearward).

The chart shows that the risk increases rapidly for backrest inclination angles above 45°. Also the risk is generally increased by about 50% for a seat position 300 mm further rearward compared to the base position.

Finite element simulations to aid plausibility checks

Individual simulations within a generic vehicle model, based on the detailed finite element model of a mid-size sedan, were set up in order to perform simple plausibility checks for some of the points on the overall risk chart. It was modelled to fit the vehicle characterisation on which the risk distributions shown in above are based. A THUMS v. 4.02 was used to model the occupant. All simulations were performed with LS-DYNA R9.2.0 (Rev. 119543) on a Linux cluster at Graz University of Technology. A view of this model is shown in Figure 16 (only the skeleton with a semi-transparent skin is visualised in this picture to aid belt path analysis).

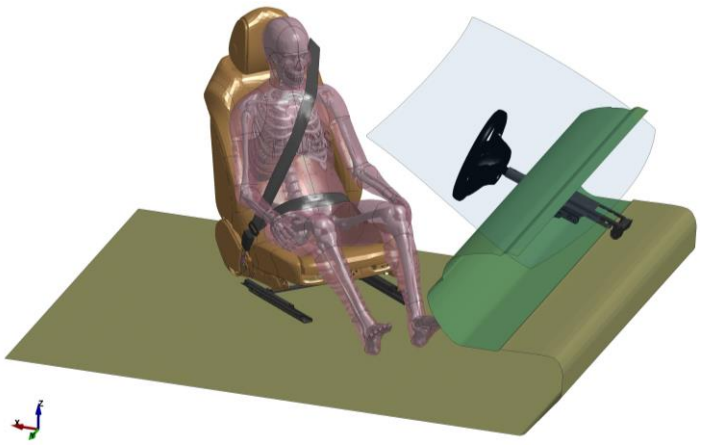

Figure 16. The THUMS v. 4.02 in the generic finite element model with the seat adjusted 300mm towards the rear and rotated by 45°.

In the following discussion, the results of these simulations are compared to the estimation of the preliminary occupant injury risk distributions shown in Figure 15 and the three severity charts (frontal/lateral/rear load case) on which the combined risk chart is based.

DISCUSSION

The comparison of the results obtained with the approach presented in this study and the results from HBM simulations in a generic virtual vehicle model suggest that the estimated preliminary occupant injury risk distributions are plausible.

For the frontal load case, the seatback inclination angles above 40° and increased distances from the frontal airbag system are not ideally covered by current state-of-the-art restraint systems. This seems to be in line with the findings of Kitagawa et al. [31], who presented still images of simulations with recline angles between 24° and 48° without an interior (and therefore without leg support). Submarining occurred in almost all of these cases. The risk charts also suggest that moderate seat rotations (30° or less) seem less problematic, given that there is sufficient leg support. This fits results obtained with the FEA with the HBM which show very similar injury risks for load directions of 0° and 15°. Apart from a 50% increase in BrIC-induced AIS^{3+}-injury risk compared to the 15° position, also the 30° position shows basically the same injury risk values. The simulations also highlighted the importance of the interior dimensions since – similar to Kitagawa et al. [31] – the HBM contacted the windscreen in the frontal load case, when the seat was rotated by 180°.

Since 30° seat rotation is the maximum value which is geometrically possible in the present interior, no significant lateral loading is observed apart from the lateral load case. This load case is currently being re-modelled to incorporate a realistic representation of the intrusions into the cabin. Since there are currently no publications available which present simulation results to compare the risk distribution to, this load case needs to be discussed in more detail once the simulation model is updated. The tendency of increased risk for even slightly increased rotation seems reasonable though, since the occupant's head is significantly closer to the side where the vehicle is struck. Considering intrusions should increase this trend. The increased risk for more or less fully rotated seats (right side in Figure 13) also seems plausible, since the side airbag is only available on the left side of the seat.

For the rear load case, the severity chart in Figure 14 suggests that seatback inclination angles up until 35° are easily feasible – even for seat rotation angles of 15°. Comparing this to the results of Zhao et al. [36] and the FEA conducted for this study, this is not entirely plausible. Zhao et al. found the highest BrIC values for loading angles in the range between 120° and 210° degrees. In the FEA, the BrIC-induced AIS^{3+}-injury risk of the head is increased significantly for 15° seat rotation ($\varphi = 195°$). This needs further investigation, since it is expected, that there is significant influence of the head restraint geometry. Also the trigger times for the seatbelt pretensioners in the FEA seem to be of vital importance – but they cannot be accounted for in the presented approach.

In summary, the approach – in its current implementation – helps to identify key combinations of load cases and interior configurations in which a given set of restraint systems. These can later be the focus of more detailed analyses. The approach can also be used as a preliminary check for feasibility in terms of the basic physical limits. Furthermore, it enables a relative comparison between different concepts (restraint systems, geometric constraints etc.) comparable to a high dimensional occupant load criterion. In this respect it also allows a preliminary estimation of the necessary effort for implementation.

LIMITATIONS

The present study has some limitations. Seat rotation was only considered about a discrete axis, while rotating seats could also swivel and move to the side to allow greater rotation angles in the confined interior space of a vehicle. Also, while different seatback inclination angles were considered the seat cushion angle was not altered. It is likely that seats offering reclining angles above 45° will also alter the seat cushion angle accordingly to provide a comfortable seat position. The occupant posture itself was not considered as a variable. In reality, occupants can take many different postures for any given seat position. A variation of the method could also include the expected distribution or field data of the most relevant seat configurations in order to weight the configurations with higher relevance from an acceptance point of view. The seat could also be moved into a safer position during the pre-crash phase [32], which was not investigated in the present study. To further reduce the loads on the occupants, the seat could be mounted in such a way that energy is dissipated between the seat and the vehicle [33]. This way, less energy is transferred to the occupant. Another area of possible improvement is the representation of intrusions into the cabin. Currently, intrusions are not considered even though they can be significant; particularly in lateral collisions. The approach can also not account for anomalies like submarining. Likewise, configurations which lead to a problematic belt path (e.g. belt slipping off the thorax and up the neck of the occupant) are not detected. While

it is theoretically possible to try to account for these issues via modifiers, it is questionable that all effects can be incorporated. It seems far more reasonable to practise due care when interpreting the resulting charts.

CONCLUSIONS

In this paper a method is presented to quickly highlight key combinations of seat configurations and crash load directions for any given interior layout and set of restraint systems in order to facilitate the evaluation of restraint systems' effectiveness. Estimating preliminary occupant injury risks for future HAVs provides an insight to their expected performance which highlights key parameter combinations and can aid the development of relevant regulations and test procedures. Finally, a first comparison of achieved results with in-depth FE simulations with a HBM showed plausible results and emphasised the validity of this approach in a well-defined range of operation. This method has shown its capability for time and resource efficient preparation of simulation studies concerning the occupant safety of future HAVs.

The presented approach helps to highlight areas in which current restraint systems reach their limits. It is based on a combination of the restraint potential and the mean deceleration for each considered configuration. The overall restraint potential combines the estimates of the individual restraint systems abilities to restrain the occupant while the mean deceleration is estimated based on the impact velocity and the space available for energy dissipation. Both measures are dependent on the seat configuration, interior geometry and load direction and therefore individually evaluated for any combination of the respective parameters. Since more complex effects like submarining can currently not be detected with this approach, they still need to be addressed separately. Nevertheless, the analysis suggests that the current occupant restraint systems need to be adapted or supplemented to ensure ideal occupant safety for increased longitudinal adjustments and more reclined backrest configurations. Moderate seat rotations (less than 30°) on the other hand, seem to be feasible with currently available restraint systems, especially if the headrest design minimises the head rotation in rear-end crashes.

The other aim was to facilitate the evaluation of restraint systems active principles. A visual assessment of the 3D-plots of the individual restraint systems' restraining potential (e.g. Figure 9), clearly shows the restraints system's dependency on the seat configuration. This could help to motivate new active principles by highlighting areas in which current systems lack performance.

Still more work is needed to validate the preliminary occupant injury risk distributions with detailed finite element simulations. This is particularly important with regards to lateral collisions, which are much more complex to model, due to the intrusions into the cabin.

The proposed approach should not be seen as a replacement for detailed finite element analyses but as a useful supplement for time and resource efficient preparation of simulation studies concerning the occupant safety of future HAVs.

ACKNOWLEDGEMENTS

This work was supported by Tech Center i-protect. The authors would also like to acknowledge the use of HPC resources provided by the ZID of Graz University of Technology.

REFERENCES

[1] National Highway Traffic Safety Administration, 2008. National Motor Vehicle Crash Causation Survey: Report to Congress. DOT HS 811 059.

[2] Statistik Austria, 2018. Straßenverkehrsunfälle Jahresergebnisse 2017: Straßenverkehrsunfälle mit Personenschaden. Wien.

[3] Sofia Jorlöv, Katarina Bohman, Annika Larsson, 2017. Seating Positions and Activities in Highly Automated Cars – A Qualitative Study of Future Automated Driving Scenarios. In: International Research Council on the Biomechanics of Injury, editor. 2017 IRCOBI Conference Proceedings. IRCOBI.

[4] Bengtsson O., 2017. Autonomous Vehicle Seats: A User Oriented Concept Design [Bachelor Thesis]. Gothenburg, Sweden: Chalmers University of Technology.

[5] International Organisation for Standardisation, 1978. Road Vehicles - Three-Dimensional Reference System and Fiducial Marks - Definitions. Geneva: International Organization for Standardization.

[6] U.S. Department of Transportation, National Highway Traffic Safety Administration, 2017. Automated Driving Systems 2.0: A Vision for Safety.

[7] Favarò F.M., Nader N., Eurich S.O., Tripp M., Varadaraju N., 2017. Examining Accident Reports Involving Autonomous Vehicles in California. PLoS ONE 12(9). https://doi.org/10.1371/journal.pone.0184952.

[8] Euro NCAP, December 2017. Pedestrian Human Model Certification. 1st ed.(TB 024); Available from: https://cdn.euroncap.com/media/34544/tb-024-pedestrian-human-model-certification-v101.pdf.

[9] C26 | Volvo Cars: Introducing a new symbol of automotive freedom. [January 28, 2019]; Available from: https://www.volvocars.com/intl/cars/concepts/c26.

[10] NIO GmbH. NIO Deutschland - Experience EVE. [January 28, 2019]; Available from: https://www.nio.io/de_DE/visioncar-experience.

[11] Adient plc. Adient unveils new luxury seating concept for level-3 and level-4 automated driving systems. [January 28, 2019]; Available from: https://www.adient.com/media/press-releases/2017/01/09/adient-unveils-new-luxury-seating-concept-for-level-3-and-level-4-automated-driving-systems.

[12] NHTSA, 2008. FMVSS Test Procedure 208-14 - Appendix A: Part 572E (50th Male) Dummy Performance Calibration Test Procedure.

[13] Hynd D., Page M., Bortenschlager K., Been B., van Ratingen M., Pastor C. et al., 2004. Status of side impact dummy developments: WorldSID development. Report number: EEVC WG12 doc 252.

[14] Davidsson J., December 30, 1999. BioRID II Final Report. Gothenburg, Sweden.

[15] Hynd D., Depinet P., Lorenz B., 2013. The repeatability and reproducibility of the BioRID IIg in a repeatable laboratory seat based on a production car seat. Traffic Inj Prev 14 Suppl:95-104. https://doi.org/10.1080/15389588.2013.806987.

[16] Newby N., Somers J.T., Caldwell E.E., Perry C., Littell J., Gernhardt M., 2013. Assessing Biofidelity of the Test Device for Human Occupant Restraint (THOR) Against Historic Human Volunteer Data. In: SAE Technical Paper Series. SAE International, 400 Commonwealth Drive, Warrendale, PA, United States.

[17] Rangarajan N., Shams T., Artis M., Huang T.J., Haffner M., Eppinger R.H. et al., 2000. Oblique and Side Impact Performance of the THOR Dummy. In: International Research Council on the Biomechanics of Injury, editor. 2000 IRCOBI Conference Proceedings. IRCOBI, p. 31–40.

[18] Somers J.T., Newby N., Lawrence C., DeWeese R., Moorcroft D., Phelps S., 2014. Investigation of the THOR Anthropomorphic Test Device for Predicting Occupant Injuries during Spacecraft Launch Aborts and Landing. Front Bioeng Biotechnol 2. https://doi.org/10.3389/fbioe.2014.00004.

[19] Kitagawa Y., Yasuki T., 2014. Development and Application of THUMS Version 4. In: CARHS, editor. 5th International Symposium: Human Modeling and Simulation in Automotive Engineering. carhs.

[20] Schap J.M., Koya B., Gayzik F.S., 2019. Objective Evaluation of Whole Body Kinematics in a Simulated, Restrained Frontal Impact. Ann Biomed Eng 47(2):512–23. https://doi.org/10.1007/s10439-018-02180-2.

[21] Park G., Kim T., Panzer M.B., Crandall J.R., 2016. Validation of Shoulder Response of Human Body Finite-Element Model (GHBMC) Under Whole Body Lateral Impact Condition. Ann Biomed Eng 44(8):2558–76. https://doi.org/10.1007/s10439-015-1546-6.

[22] Katagiri M., Zhao J., Lee S., Kang Y.-S., Nov. 2018. GHBMC M50-O Occupant Response in Moderate-Speed Rear Impacts. 46th International Workshop on Human Subjects for Biomechanical Research.

[23] Fressmann D., June 2016. The THUMS Human Models: Overview. Infotag Human Modeling. Stuttgart.

[24] Hwang E., Hu J., Chen C., Klein K.F., Miller C.S., Reed M.P. et al., 2016. Development, Evaluation, and Sensitivity Analysis of Parametric Finite Element Whole-Body Human Models in Side Impacts. In: The Stapp Association, editor. Stapp Car Crash Journal. Warrendale, PA, United States: SAE International.

[25] Kato D., Nakahira Y., Atsumi N., Iwamoto M., 2018. Development of Human-Body Model THUMS Version 6 containing Muscle Controllers and Application to Injury Analysis in Frontal Collision after Brake Deceleration. In: International Research Council on the Biomechanics of Injury, editor. 2018 IRCOBI Conference Proceedings. IRCOBI.

[26] Kimpara H., Nakahira Y., Iwamoto M., 2016. Development and Validation of THUMS Version 5 with 1D Muscle Models for Active and Passive Automotive Safety Research. Conference Proceedings: Annual International Conference of the IEEE Engineering in Medicine and Biology Society:6022–5. https://doi.org/10.1109/EMBC.2016.7592101.

[27] Iwamoto M., Nakahira Y., Kimpara H., 2015. Development and Validation of the Total HUman Model for Safety (THUMS) Toward Further Understanding of Occupant Injury Mechanisms in Precrash and During Crash. Traffic Inj Prev 16 Suppl 1:48. https://doi.org/10.1080/15389588.2015.1015000.

[28] Panzer M.B., Giudice J.S., Parent D., January 2015. THOR 50th Male Finite Element Model User Manual: Model Version 2.1 for LS-Dyna.

[29] Stahlschmidt S., Huang Y., Usta E., February 9, 2018. Documentation PDB LS-Dyna WorlSID 50th - Version 5: User's Manual Release 0.0 for Model v5.0. Germany.

[30] Klug C., 2018. Assessment of Passive Vulnerable Road User Protection with Human Body Models [Doctoral Thesis]. Graz: Graz University of Technology.

[31] Kitagawa Y., Hayashi S., Yamada K., Gotoh M., 2017. Occupant Kinematics in Simulated Autonomous Driving Vehicle Collisions: Influence of Seating Position, Direction and Angle. In: The Stapp Association, editor. Stapp Car Crash Journal. Warrendale, PA, United States: SAE International, p. 101–155.

[32] Jin X., Hou H., Shen M., Wu H., Yang K.H., 2018. Occupant Kinematics and Biomechanics with Rotatable Seat in Autonomous Vehicle Collision: A Preliminary Concept and Strategy. In: International Research Council on the Biomechanics of Injury, editor. 2018 IRCOBI Conference Proceedings. IRCOBI.

[33] Huf A., Sengottu Velavan S., 26.11 - 28.11.2018. Development of Occupant Restraint Systems for Future Seating Positions in Fully or Semi-Autonomous Vehicles. In: Fraunhofer ICT, editor. Airbag 2018: 14th International Symposium & Accompanying Exhibition on Sophisticated Car Safety Systems.

[34] Lin H., Gepner B., Wu T., Forman J., Panzer M., 2018. Effect of Seatback Recline on Occupant Model Response in Frontal Crashes. Short Communication. In: International Research Council on the Biomechanics of Injury, editor. 2018 IRCOBI Conference Proceedings. IRCOBI.

[35] Gepner B., Lin H., Wu T., Forman J., Panzer M., January 24-26, 2018. The Challenge of Out of Position Occupants for Passive Safety in Automated Vehicles.

[36] Zhao J., Katagiri M., Lee S., Hu J., 2018. GHBMC M50-O Occupant Response in A Frontal Crash of Automated Vehicle. In: CARHS, editor. 7th International Symposium: Human Modeling and Simulation in Automotive Engineering.

[37] Boin M., 2018. Occupant Protection in Alternative Seating Positions. In: DYNAmore, editor. 15th German LS-DYNA Forum.

[38] Hillenbrand M., 2011. Funktionale Sicherheit nach ISO 26262 in der Konzeptphase der Entwicklung von Elektrik/Elektronik Architekturen von Fahrzeugen [Doctoral Thesis]. Hannover, Karlsruhe.

APPENDIX

Table 3.
Values for the parameters used to characterise the vehicle interior and load cases in the present study.

Parameter	Value	Unit	Comments
occDistHeadPelvis	0,67	m	Distance H-point to COG head
spaceBasePositionX	0,40	m	Initially available deceleration space - frontal
spaceBasePositionY	0,50	m	Initially available deceleration space - lateral
spaceBasePositionMinusX	1,00	m	Initially available deceleration space - rear
spaceAvailableY	0,50	m	Available space to the side (for seat rotation)
seatDepthBehindHead	0,20	m	Distance between COG head and rearmost part of the seat
seatBackWidth	0,35	m	Seatback width (at rearmost part)
velocityFront	15,56	m/s	Impact velocity - frontal
velocitySide	8,33	m/s	Impact velocity - side
velocityRear	11,11	m/s	Impact velocity - rear